Published in final edited form as:
Neuron. 2015 January 7; 85(1): 101–115. doi:10.1016/j.neuron.2014.11.018.

NFκB-activated Astroglial Release of Complement C3 Compromises Neuronal Morphology and Function Associated with Alzheimer's Disease

Hong Lian[1,2], **Li Yang**[1], **Allysa Cole**[1], **Lu Sun**[1], **Angie C.-A. Chiang**[3], **Stephanie W. Fowler**[3], **David J. Shim**[1,3], **Jennifer Rodriguez-Rivera**[1], **Giulio Taglialatela**[4], **Joanna L. Jankowsky**[1,3], **Hui-Chen Lu**[3,5], and **Hui Zheng**[1,2,3,*]

[1]Huffington Center on Aging, Baylor College of Medicine, Houston, Texas 77030, USA

[2]Department of Molecular and Human Genetics, Baylor College of Medicine, Houston, Texas 77030, USA

[3]Department of Neuroscience, Baylor College of Medicine, Houston, Texas 77030, USA

[4]Departments of Neuroscience and Cell Biology, University of Texas Medical Branch, Galveston, Texas 77555, USA

[5]Department of Pediatrics, Baylor College of Medicine and the Cain Foundation Laboratories, Jan and Dan Duncan Neurological Research Institute at Texas Children's Hospital, Houston, Texas 77030, USA

SUMMARY

Abnormal NFκB activation has been implicated in Alzheimer's disease (AD). However, the signaling pathways governing NFκB regulation and function in the brain are poorly understood. We identify complement protein C3 as an astroglial target of NFκB, and show that C3 release acts through neuronal C3aR to disrupt dendritic morphology and network function. Exposure to Aβ activates astroglial NFκB and C3 release, consistent with the high levels of C3 expression in brain tissue from AD patients and APP transgenic mice, where C3aR antagonist treatment rescues cognitive impairment. Thus, dysregulation of neuron-glia interaction through NFκB/C3/C3aR signaling may contribute to synaptic dysfunction in AD and C3aR antagonists may be therapeutically beneficial.

Keywords

Alzheimer's disease; astroglia; behavior; complement pathway; C3a receptor; dendritic morphology; IκBα; intraneuronal calcium; mice; neuron-glia signaling; NFκB; surface AMPA receptor

*Correspondence: huiz@bcm.edu.

INTRODUCTION

Astroglia are responsible for diverse functions in the central nervous system (CNS) and play a crucial role in maintaining neuronal physiology. Astroglia maintain glucose, ATP, and glutamate homeostasis, modulate synaptic formation and function, and are an essential component of the blood brain barrier (Coulter and Eid, 2012; Lalo et al., 2014; Seifert and Steinhauser, 2013). In response to brain insults such as injury, infection, or neurodegeneration, astroglia become reactive, and these are associated with the activation of immune mediators and release of proinflammatory cytokines (reviewed by (Kyritsis et al., 2014)). A key regulator of inflammation in the peripheral system and CNS is the hetero-dimeric transcription factor nuclear factor-kappa B (NFκB) (reviewed by (Baltimore, 2011; Oeckinghaus and Ghosh, 2009)). Under normal conditions, NFκB is tightly regulated by its inhibitor protein IκB which sequesters NFκB in the cytoplasm. Upon degradation of IκB, NFκB translocates to the nucleus where it activates expression of κB target genes, including its inhibitor IκBα (Chiao et al., 1994) to form an autoinhibitory feedback loop that ensures proper silencing of NFκB following each activation. Accordingly, deletion of *IκBα* (Beg et al., 1995; Klement et al., 1996) or disruption of the κB sites in the *IκBα* promoter (Peng et al., 2010; Shim et al., 2011) leads to aberrant NFκB activation and a spectrum of immunological phenotypes.

Activation of NFκB is associated with various neurodegenerative conditions including Alzheimer's disease (Kaltschmidt et al., 1997; Mori et al., 2010), Parkinson's disease (Hunot et al., 1997), and Huntington's disease (Hsiao et al., 2013). Both neurotoxic and neuroprotective roles have been proposed for NFκB, with the outcome likely dependent on the timing, duration, and level of activity (reviewed by (Mattson et al., 2000; Mattson and Meffert, 2006; Pizzi and Spano, 2006)). Given the potential importance of aberrant NFκB activation in neuroinflammatory conditions, it is important to clarify the signaling cascades mediating its activity in neurons and glia and to understand the conditions under which NFκB either attenuates or aggravates disease.

The complement pathway is an essential immune regulator of host defense to infection, cell integrity, and tissue homeostasis in the peripheral system (Holers, 2014; Ricklin and Lambris, 2013). Full complement activation involves concerted actions of over 30 proteins that participate in three distinct pathways: classical, alternative, and mannose-binding-lection (MBL); all converge on the cleavage of the central complement protein C3 (Zipfel and Skerka, 2009). In the CNS, complement factors such as C3a and C1q have been shown to regulate synaptic refinement and neuronal survival during development (Benoit and Tenner, 2011; Shinjyo et al., 2009; Stevens et al., 2007). However, little is known about the mechanisms regulating complement expression and its influence on neuronal function and dysfunction in the adult brain.

Here we examined the cell-specific effects of NFκB activation in neurons or astroglia by deleting its inhibitor IκBα in these cell types. We identify a novel neuron-glia interaction pathway whereby astroglial NFκB activation and subsequent release of complement C3 acts through neuronal C3a receptor to impair dendritic structure and network function.

RESULTS

Complement factor C3 is an astroglial target of NFκB

We created a CNS-specific *IκBα* deletion (NcKO) by crossing an *IκBα* floxed allele with a Nestin-Cre transgenic line (Lian et al., 2012). Consistent with its role as a principal inhibitor of NFκB, we found that deletion of IκBα was associated with sustained NFκB activity (Lian et al., 2012). We performed expression profiling of hippocampal samples taken from the NcKO mice and their littermate controls to identify downstream targets activated by NFκB (Figure S1A). Among the many genes identified, we found that complement factor 3 (C3), a central molecule in the complement signaling pathway, was significantly upregulated in the NcKO mice (Figure S1A and Figure 1A).

We and others have previously shown that astrocytes display prominent NFκB activity (Herkenham et al., 2011; Lian et al., 2012; Mao et al., 2009). Consistent with an astrocytic bias in NFκB signaling, we found that IκBα, a known downstream target of NFκB, was expressed at substantially higher levels in astroglia than in neurons under both basal (~5-fold) and TNFα-stimulated conditions (~50-fold) (Figure S1B). TNFα induced drastic IκBα upregulation in astroglia but only marginal induction in neurons (Figure S1B). These results establish that astroglia, rather than neurons, are the main site of IκBα expression and NFκB activity.

The prominent NFκB response in astroglia suggests that the rise in hippocampal C3 expression observed in the NcKO mice likely originated from astroglia. To test this prediction, we crossed the *IκBα* floxed allele with CaMKIIα-Cre (Dragatsis and Zeitlin, 2000) or GFAP-Cre (Bajenaru et al., 2002) to create mice with selective *IκBα* deletion in neurons (CcKO) or in astrocytes (GcKO), respectively (Figure S1C). Astroglial deletion of *IκBα* reduced the level of IκBα mRNA and protein by roughly the same amount as the whole brain knockout, confirming that the majority of NFκB signaling was indeed localized to astrocytes (Figures S1D and S1E). C3 mRNA expression in the astrocyte-specific GcKO, but not the neuron-specific CcKO, also matched that of whole-brain NcKO (Figure 1A). ELISA analysis confirmed elevation of C3 protein levels in the GcKO mice (Figure 1B). As with whole brain IκBα deletion, no overt phenotypes were detected in the GcKO mice (Figure S1F).

The *C3* promoter contains two putative κB binding sites (Figure S1G) and is speculated to be an NFκB target (Moon et al., 1999; Vik et al., 1991). To test whether *C3* transcription is mediated by direct binding of NFκB to the *C3* promoter, we performed chromatin immunoprecipitation (ChIP) in primary astroglial cultures using an anti-p65 antibody to recover DNA bound to NFκB in the presence and absence of TNFα stimulation. PCR analysis showed that while the κB-1 site was enriched in all immunoprecipitates, the κB-2 site was enriched only upon TNFα stimulation (Figures S1G and S1H). While the reason for the differential response to TNFα remains to be established, this result validated C3 as a direct NFκB target in astroglia.

The GFAP-Cre line can evoke neuronal deletion of floxed alleles (Bajenaru et al., 2002; Drögemüller et al., 2008), so we employed a second strategy to confirm that astrocytes were

selectively responsible for C3 elevation following NFκB activation. We prepared primary astroglial and neuronal cultures derived from germline *IκBα* knockout mice (KO) and their littermate wild-type (WT) controls (Beg et al., 1995). In agreement with the in vivo data, we detected ~10-fold higher basal C3 mRNA levels in WT astroglial cultures compared to the WT neuronal cultures (compare WT Astroglia vs. WT Neuron, Figure 1C). Significantly, IκBα deletion did not affect C3 expression in neuronal cultures (compare KO Neuron vs. WT Neuron, Figure 1C), but led to an approximately 3-fold further increase in astroglia (compare KO Astroglia vs. WT Astroglia, Figure 1C). Increased astroglial C3 in the absence of IκBα was further confirmed by normalizing C3 mRNA with other house-keeping genes (Figures S1I and S1J) and by measuring secreted C3 protein in conditioned media of WT and IκBα KO astroglial cultures (Figure 1D).

To confirm that C3 overexpression in IκBα mutants is dependent on NFκB, we applied the NFκB inhibitor JSH23 to WT and IκBα KO primary astroglial cultures in the presence or absence of TNFα. We found that C3 mRNA levels were not affected by JSH23 in WT cultures, but both basal and TNFα-induced C3 upregulation was potently blunted by JSH23 in IκBα KO astrocytes (Figure 1E). We noticed a small but significant increase of C3 in WT cultures in response to TNFα stimulation (Figure 1E, WT, − vs. + TNFα), however, this pool was insensitive to JSH23, suggesting that other transcriptional modulators, such as C/EBP or MAPK, were responsible for the increase (Maranto et al., 2008, 2011). Taken together, our in vivo and in vitro data provide unequivocal support that astroglia, rather than neurons, are the principle site of NFκB activation and primarily responsible for the NFκB-dependent increase in C3.

Given that C3 is a central molecule in the complement signaling cascade, we tested which complement pathway is activated by C3 overexpression. We measured the mRNA of proteins required for classical (C1q and C4) or alternative (Cfb and Cfh) complement pathways in WT and IκBα-deficient astroglial cultures (Figure S1K) and mouse brains (Figure S1L). We detected upregulation of classical complement factors C1q and C4 but not alternative pathway factors Cfb or Cfh. These results suggest that astroglial NFκB/C3 promotes activation of the classical complement pathway.

Astroglial NFκB/C3 activation leads to impaired synaptic density and dendritic morphology

We next wanted to explore what impact astrocytic C3 release might have on the structure or function of neighboring neurons. We employed a co-culture system of primary WT or IκBα knockout astroglia (WTA or KOA respectively) with WT hippocampal neurons to measure synaptic density and dendritic morphology in the presence or absence of astroglial NFκB activation. Double immunostaining of these cultures with NeuN/Iba1 (Figure S2A) or GFAP/Iba1 (Figure S2B) revealed that microglia comprises less than 1% of the total cell population in both neuronal and astrocytic cultures (Figure S2C), arguing against a potential contribution of microglia in the culture system.

Synaptic density was evaluated by co-immunostaining for the synaptic marker synaptophysin (Syn) and the dendritic microtubule-associated protein 2 (MAP2) (Figure 2A). We found significant reduction of synaptic density in WT neurons co-cultured with

IκBα KO astroglia (Figure 2C). Further examination of excitatory and inhibitory synapses using vesicular glutamate transporter 1 (VGluT1, Figure 2B) or vesicular GABA transporter (VGAT, Figure S2D), respectively, revealed significant reduction in excitatory but not inhibitory synapses (Figure 2C). In addition, both total dendritic length (Figure 2D) and dendritic complexity (Figures 2E and 2F) were reduced in neurons plated with IκBα KO astrocytes.

To test that the neuronal phenotypes triggered by IκBα KO astroglia were mediated through C3, we supplemented WT neuronal monocultures with different doses (1, 2, 5 μg/ml) of recombinant C3 and determined the effect on neuronal morphology. Similar to neurons cultured with KO astrocytes, both the synaptic density (Figures 2G and 2H) and dendritic complexity (Figures 2I and 2J) were reduced at all C3 concentrations tested. Conversely, we tested whether immunodepletion of C3 from conditioned media derived from IκBα KO astroglia would abrogate its impact on neuronal morphology. Neurons treated with C3-depleted, but not GFP-depleted media, maintained normal dendritic morphology (Figures S2H and S2I). These experiments support a role for secreted C3 in mediating the effects of astroglial NFκB activation on neuronal morphology.

To corroborate these findings in vivo, we used AAV to sparsely label cortical neurons with GFP in adult WT and astroglial IκBα–deficient (GcKO) mice (Figure 3; Movie S1). We reconstructed the 3D structure of dendritic segments to perform unbiased automatic classification of spine types (mushroom, stubby, long-thin, and filopodia) (Figure 3A). With the exception of filopodia, all other spine types (Figures 3C and S3B) as well as total spine density (Figures 3B and S3A) were significantly reduced in the GcKO mice, without altering the relative percentage of each spine type (Figures 3D and S3C).

Neuronal complement receptor C3aR mediates the effect of astroglial NFκB/C3 signaling

We next wanted to test whether neuronal complement receptor was required to translate astrocytic C3 release into a neuronal morphological response. Cleavage of C3 generates C3a and C5a, which executes complement functions through binding of its receptor C3aR and C5aR, respectively (Nataf et al., 1999; Rahpeymai et al., 2006). C3aR and C5aR are both G-protein coupled receptors expressed in many cell types including neurons (Bénard et al., 2008; Gasque et al., 2000; Shinjyo et al., 2009). We tested whether C3aR or C5aR were neuronal mediators of the NFκB/complement pathway by treating neuron-astrocyte co-cultures with antagonists against C3aR (C3aRA) or C5aR (C5aRA). We again used WT neurons cultured with either WT or IκBα KO astrocytes in the presence or absence of these complement receptor antagonists. Sholl analysis revealed that blocking C3aR, but not C5aR, preserved dendritic branching and spine density in the KOA cultures (Figures 4A, 4B, and S4A-S4E). Whereas C3aR antagonist increased dendritic complexity in neurons cultured with KO astrocytes (Figure 4B, KOA, DMSO vs. C3aRA), it had an apparent opposite effect on neurons cultured with WT astrocytes (Figure 4B, WTA, DMSO vs. C3aRA). These results suggest that while excessive C3/C3aR activity is detrimental to neuronal health, basal C3aR signaling might play a role in maintaining normal dendritic extension.

C3aR is expressed in both neurons and astroglia and, thus, it is plausible that astroglial C3aR may have contributed to the effects of C3aR manipulation in our co-culture system. To rule

out this possibility, we tested whether loss of neuronal C3aR would abrogate dendritic phenotypes when cultured with IκBα KO astrocytes. We again performed co-culture experiments with IκBα KO astrocytes, but used neurons derived from WT (C3aRWTN) or C3aR null (C3aRKON) mice (Humbles et al., 2000) (Figures 4C and 4D). We found that dendritic complexity in neurons cultured with IκBα KO astrocytes was preserved by neuronal C3aR deletion (Figure 4D), thus establishing a definitive role of neuronal C3aR in the response to astroglial C3 release. Unlike the C3aRA treatment, although there is a trend of reduction in dendritic extension in C3aR knockout neurons, the difference did not reach statistical significance (compare C3aRWTN WTA with C3aRKON WTA, Figure 4D). Possible compensation resulting from germline C3aR-deficiency may be a contributing factor for the differences between pharmacological inactivation and genetic ablation.

To provide in vivo evidence that C3aR is required for the observed effects of astroglial NFκB activation, we treated WT and astroglial IκBα KO (GcKO) mice systemically with C3aR antagonist (Figures 4E and 4F). AAV was again used to sparsely label cortical neurons with GFP so spine density could be measured following 3 weeks of antagonist or vehicle treatment. While C3aRA treatment had no significant effect on WT animals (Figures 4F and S4F, Ctrl, DMSO vs. C3RA), it completely rescued spine density in GcKO mice (Figures 4F and S4F, GcKO, DMSO vs. C3aRA). Taken together, these results demonstrate that abnormal C3/C3aR signaling affects neuronal morphology in vitro and in vivo.

The above studies identified a novel pathway by which astroglial NFκB activation leads to elevated complement signaling and reduced synaptic and dendritic densities in vitro and in vivo. These were correlated with neuronal circuitry deficits as the IκBα GcKO mice exhibit impaired hippocampal-dependent contextual fear response (Figure 4G) and long-term potentiation (LTP) of the Schaffer collateral pathway (Figure 4I). Consistent with the rescue of dendritic morphology by C3aR blockade, both the behavioral and synaptic plasticity deficits were attenuated by C3aR antagonist treatment (Figures 4H and 4J).

Intraneuronal calcium mediates neuronal excitation downstream of C3aR

It has been reported that C3aR hyperactivation can mobilize intracellular calcium in some cell types (Ahamed et al., 2004; Murakami et al., 1993; Sayah et al., 2003). Calcium dysregulation could in turn initiate a cascade of changes ultimately leading to alteration of neuronal morphology and function. We examined intraneuronal calcium flux in both astrocyte-neuron co-cultures and brain slice cultures with the fluorescent reporter GCaMP6 (Chen et al., 2013). WT neurons cultured with IκBα KO astrocytes (KOA) showed substantially higher baseline calcium levels than neurons cultured with WT astrocytes (Figures 5A and B). We observed similar elevation in baseline calcium of GcKO slice cultures compared to littermate controls (Figures 5C and 5D). Baseline calcium levels were restored to normal both by application of the calcium chelator BAPTA/AM or C3aRA to the cultured slices, suggesting that calcium dysregulation was downstream of C3aR signaling (Figure 5E). Finally, normalizing calcium levels with BAPTA/AM (Figure 5E) rescued dendritic morphology in neurons cultured with IκBα KO astrocytes (Figures 5F and 5G), placing intraneuronal calcium in the pathway leading from activated NFκB to altered neuronal morphology.

The above studies established a novel function of astroglial NFκB, through C3/C3aR signaling and intraneuronal calcium regulation, in mediating excitatory synaptic density and dendritic morphology. We next performed electrophysiological recordings of excitatory synaptic transmission in neurons co-cultured with WT or IκBα KO astrocytes. We observed miniature EPSCs of larger amplitude in neurons cultured with IκBα KO astrocytes than with WT astrocytes, despite no change in frequency, indicating that synaptic strength was increased by astroglial NFκB/C3 signaling (Figures 6A-6D). The strength of postsynaptic events is controlled predominantly by AMPA receptor (AMPAR) trafficking (Derkach et al., 2007; Song and Huganir, 2002; Yamada, 1998), so we performed immunocytochemical staining of AMPAR subunit GluR1 to examine its surface expression (Figure 6E). Compared with the WT co-cultures, neurons cultured with IκBα KO astrocytes displayed higher surface GluR1 intensity both generally at the cell membrane (Figure 6F) and specifically within synaptophysin-positive (Syn^+) puncta (Figure 6G). In contrast, total GluR1 intensity was not changed, both when measured by immunostaining of co-cultured neurons (Figures S5A and S5B) and by Western blot using lysates from co-cultured neurons or GcKO brains (Figures S5C-S5F). Increased surface GluR1 was further validated by Western blotting of biotinylated cell surface GluR1, which showed a significant upregulation in neurons cultured with IκBα KO astrocytes (Figures 6H and 6I). These data suggest that astroglial NFκB activation results in significant enrichment of AMPAR at the postsynaptic surface.

Consistent with the prominent rescue of spine density in vitro and in vivo by C3aR inhibition, application of C3aRA to WT neurons cultured with IκBα KO astrocytes normalized mEPSC amplitude (Figures 6J and 6K) as well as surface AMPAR expression (Figures 6L and 6M). Diminished levels of surface AMPAR were observed within 15 minutes of C3aRA treatment (Figures S5G) strongly supporting a direct effect of C3/C3aR signaling. Similar to C3aRA, treatment with BAPTA/AM also rescued surface GluR1 expression in neurons cultured with KO astrocytes (Figure 6N), supporting the idea that intraneuronal calcium mediates AMPAR trafficking downstream of astroglial NFκB/C3.

Alterations of NFκB and C3 levels by Aβ and in AD brains

Substantial evidence has implicated dysregulation of NFκB and calcium homeostasis in AD pathogenesis (LaFerla, 2002; Mattson, 2007; Mattson and Meffert, 2006). To explore whether the astroglial NFκB/C3 pathway uncovered here is induced under conditions relevant to AD, we treated WT primary astroglial cultures with either the Aβ42 peptide or the control reverse peptide rAβ42. Remarkably, Aβ42, but not rAβ42, resulted in prominent translocation of NFκB from the cytoplasm to the nucleus (Figures 7A and 7B), and increased expression of C3 mRNA (Figure 7C).

We next examined whether Aβ accumulation in vivo was associated with C3 elevation, and whether inhibiting C3aR signaling could rescue cognitive impairment in amyloid-bearing mice. Consistent with the effect of Aβ in vitro, we found that C3 mRNA levels were significantly higher in APP/TTA double transgenic mice than in TTA single-transgenic controls (Figure 7D) (Jankowsky et al., 2005). We then treated mice with C3aRA or vehicle DMSO for 3 weeks before testing their performance in Morris water maze (MWM) and

radial arm water maze (RAWM) (Fowler et al., 2014). Treatment was initiated at an age when cognitive impairments are already manifested, and consistent with past characterization of this model, vehicle-treated APP/TTA mice took more days of training than TTA controls to reach criteria performance in the MWM and made more working memory errors in the RAWM (Figures 7E and 7F). Whereas C3aRA treatment did not change the behavior of control TTA mice, it improved the performance of APP/TTA mice to control levels in both tasks (Figures 7E and 7F).

To further assess whether this pathway is perturbed in human disease, we performed biochemical analysis of NFκB, IκBα, and C3 in postmortem AD brains and age-matched non-demented controls. Both NFκB, measured by nuclear p65 levels (Figure 7G) and its targets IκBα (Figures 7H and 7I) and C3 (Figure 7J) were significantly higher in AD samples than controls. Although the sequence of events leading to upregulation of NFκB signaling in AD remains to be elucidated, our findings overall support a role for altered astrocytic IκBα/NFκB signaling in AD pathophysiology.

DISCUSSION

Loss-of-function studies have revealed essential roles of NFκB and the complement system in neuronal function and synapse elimination during development (Boersma et al., 2011; Koo et al., 2010; Meffert et al., 2003; Stevens et al., 2007), However, these pathways are known to be activated under pathological conditions. Very few genetic gain-of-function models have been generated (Gerondakis et al., 2006; Hanafusa et al., 2002), and those that exist have been limited to ectopic overexpression which may not be appropriate for understanding these pathways in pathological conditions. Furthermore, little is known about cell-type specific regulation and cross-talk between the two pathways. Here we used Cre-directed *IκBα* deletion to create mice in which NFκB was selectively activated in either neurons or astroglia and combined the genetic model with neuron-astrocyte co-cultures to study the consequence of aberrant NFκB signaling in the brain. We reveal that 1) astroglia, not neurons, are the main source of IκBα-dependent NFκB activation; 2) complement factor C3 is an astroglial NFκB target that engages neuron-glia interaction through neuronal C3aR; 3) aberrant elevation of NFκB/C3/C3aR signaling alters dendritic morphology and excitatory synaptic function through intraneuronal calcium dysregulation; and 4) antagonizing C3aR restores morphological and functional defects resulting from NFκB hyperactivation. Our studies thus reveal a critical role for the astroglial IκBα/NFκB loop in neuronal homeostasis through a novel neuron-glia signaling pathway that has direct relevance for AD pathogenesis. Both NFκB and C3 are induced in astroglia by exposure to Aβ and are upregulated in APP transgenic mice and human AD tissue. This pathway may also provide a potential entry point for therapeutic intervention, as short-term C3aR inhibition produced nearly complete rescue of multiple cognitive deficits in APP transgenic mice.

NFκB/C3 mediated neuron-glia signaling in neuronal homeostasis

NFκB has been shown to regulate neuronal survival and function (Ahn et al., 2008; Kaltschmidt et al., 2006; Kassed et al., 2002; Levenson et al., 2004; Meffert et al., 2003).

These activities have been attributed, at least in part, to the presence of constitutive NFκB activity in neurons (Blondeau et al., 2001; Kaltschmidt et al., 2000; Kaltschmidt et al., 1993, 1995; Kaltschmidt et al., 1994). However, recent studies by us and others reported that, compared to astroglia, neurons exhibit negligible NFκB activity (Lian et al., 2012; Mao et al., 2009). Consistent with this assessment, we found that both IκBα and C3 are expressed at substantially higher levels in astroglia compared to neurons under both basal and TNFα-stimulated conditions. Furthermore, only astroglial, but not neuronal, C3 is regulated in an NFκB-dependent manner. Therefore, although it remains possible that other IκBs may regulate neuronal NFκB, our results provide strong support that IκBα is a critical mediator of NFκB activity in astroglia but not in neurons.

Although the current study is focused on addressing the pathological consequences of NFκB activation, the astroglial NFκB/C3-mediated neuron-glia interaction may also mediate neuronal and synaptic function under physiological conditions. For example, during early postnatal development, complement proteins including C3 and C1q are highly expressed in the brain (Stevens et al., 2007), and C3aR has been reported to regulate the migration and differentiation of neuronal progenitor cells (Rahpeymai et al., 2006; Shinjyo et al., 2009). Interestingly, NFκB is also transiently activated during neural development (Guerrini et al., 1997; Simakajornboon et al., 2001), making it tempting to speculate that NFκB serves the same function in development as in the adult brain, and in both cases it indirectly controls neural function by regulating the onset and degree of complement activity in astroglia.

Previous studies have shown that glia-derived TNFα controls neuronal synaptic strength (Beattie et al., 2002) and mediates synaptic scaling during activity blockade (Stellwagen and Malenka, 2006). In the current study, we found that TNFα increases C3 mRNA expression, and that enhanced astroglial NFκB/C3/C3aR signaling promotes AMPAR membrane localization to increase synaptic strength. Taken together, these findings raise the possibility that C3/C3aR neuron-glia signaling may act downstream of TNFα to promote synaptic plasticity.

In addition to astrocytes, NFκB and complement proteins are also abundantly expressed in microglia (Farber et al., 2009; Lucin and Wyss-Coray, 2009; Sheppard et al., 2011; Wyss-Coray and Rogers, 2012; Zhang et al., 2014). While we provide evidence for direct neuron-astroglia interaction, it is important to note that there may exist a parallel neuron-microglia interaction mediated through the same NFκB/complement pathway. Further, astrocyte-derived complement proteins may also signal microglial activation, leading indirectly to neuronal dysfunction through a myriad of microglial-derived factors. Crosstalk between microglia, astroglia, and neurons has long confounded elucidation of their individual roles in neuroinflammatory damage. The combination of genetic and co-culture approaches we used here to study neuron-astroglia interactions may provide a useful roadmap for future work on the neuron-microglia relationship.

NFκB/C3 mediated neuron-glia signaling in Alzheimer's disease

Activation of NFκB and complement are common features in AD and other neurological conditions. However, it has been difficult to establish whether NFκB and complement activation cause neuronal dysfunction or are a consequence of neuronal injury and

neuroinflammation. In the current study, we identified C3 as a *bona fide* astroglial-specific NFκB target that is both necessary and sufficient to produce neuronal impairment through C3aR and intraneuronal calcium signaling. Our data is consistent with the notion that calcium dysregulation is a major cause of defective synaptic function in multiple neurodegenerative diseases, AD in particular (LaFerla, 2002; Mattson, 2007). Overall we propose a model whereby Aβ evokes astroglial NFκB activation and release of C3 which, through neuronal C3aR and intraneuronal calcium, increases synaptic excitation and disrupts dendritic morphology, the combination of which leads to network dysfunction. This model links Aβ with synaptic defects and neuronal hyperexcitability through a novel neuron-glia signaling pathway and places the astroglial IκBα/NFκB regulatory loop and complement activation as integral events in AD pathogenesis.

C3aR antagonists as therapeutic target for AD

Our findings that the astroglial NFκB/complement levels are inducible by Aβ; that this pathway is elevated in AD mouse models and patient brain samples; and that inhibition of C3aR ameliorates the behavioral deficits in AD mouse model support the notion that inhibiting this pathway may be therapeutically beneficial. This assessment is further supported by past studies documenting a general neuroprotective effect by blocking complement activation (Fonseca et al., 2009; Leinhase et al., 2006; Woodruff et al., 2008). As a GPCR, C3aR may prove highly tractable for pharmaceutical inhibition, and importantly, mice with complete C3aR deletion are overtly normal (Humbles et al., 2000). Thus, C3aR may make an attractive target for intervention in AD.

EXPERIMENTAL PROCEDURES

Mouse models and manipulations

The mouse lines and behavioral protocols were described in Supplemental Experimental Procedures. Quantification of spine density was performed 3 weeks after bilateral stereotaxic injection of 1 μl AAV-GFP (Penn vector core, #AV-9-PV0101, 1×10^{13}TU/ml) into the mouse cortex (+2.0 mm AP, ±3.0 mm ML, −1.5 mm DV). Beginning three days following stereotaxic injection, mice were injected i.p. with 0.5% DMSO or C3aRA (1mg/kg) 3 times per week (Monday, Wednesday, and Friday) for 3 weeks. Astroglial IκBα knockout (GcKO) mice and controls at 9 or 15 months were used for behavioral testing and LTP recording. The APP/TTA mice and the TTA controls were tested at 8 months of age, following 3 weeks of C3aRA or vehicle treatment.

All animal procedures were performed in accordance with NIH guidelines and with the approval of the Baylor College of Medicine Institutional Animal Care and Use Committee.

Primary cell culture, neuron-astroglia co-culture, slice culture, and treatment

Primary neurons were prepared from P0 pups using a previously described protocol (Lian et al., 2012). Primary astroglia were cultured using the same protocol but with astroglial medium (DMEM with 10% FBS). Contaminating cells on top of astroglia monolayer were removed by overnight shaking at 220 rpm at 37°C. For co-culture, astroglial cells were seeded on matrigel-coated cell culture inserts (Costar, #3450, #3470) and transferred to

DIV1 primary neurons. 5 μM AraC was supplemented to curb glia proliferation. Co-cultures were maintained for 2 weeks before immunostaining or recording. Two independent cultures were used for all in vitro experiments.

20 μM NFκB inhibitor JSH23 (Calbiochem, #481408) and 50 ng/ml TNFα (Sigma, #T0157) were added to astroglial cultures for 20 hrs for inhibitor assay. BAPTA/AM (Calbiochem, #196419), C3 (Millipore, #204885), C3aRA (Calbiochem, #SB290157), or C5aRA (Calbiochem, #W54011) at different dosages (specified in figure legends) were added to cultures at DIV10 for long-term or at DIV14 for short-term incubation. AAV-GCaMP6s (Penn Vector Core, #AV-1-PV2824) were added to neuronal cultures at MOI of 2.41×10^{6} immediately after neurons were seeded and removed when media was replaced. Synthetic Aβ42 (Invitrogen, #03-111) and rAβ42 (Sigma #SCP0048) peptides were prepared as previously described (Stine et al., 2003) and used at 100 nM on primary astroglia for 20 min before fixation for staining or for 20hrs before cell harvest for qPCR.

Slice cultures were prepared following the protocol described in (Gogolla et al., 2006). 1 μl AAV-GCaMP6s virus at the titer of 2.41×10^{13} TU/ml was added to the media immediately before slices were plated and removed when media was replaced.

qRT-PCR and Enzyme-linked immunosorbent assay (ELISA)

cDNA was synthesized and analyzed as described previously (Yang et al., 2009). The primer sequences are:

5’-AAGCATCAACACACCCAACA-3’ (C3 Fwd); 5’-CTTGAGCTCCATTCGTGACA-3’ (C3 Rev);

5’-AATGTGTCCGTCGTGGATCTGA-3’ (GAPDH Fwd); 5’-GATGCCTGCTTCACCACCTTCT-3’ (GAPDH Rev).

C3 levels in brain lysates were determined using mouse C3 ELISA kit (Genway, #GWB-7555C7). Quantification of relative nuclear p65 level was determined using Cayman NFκB (p65) Transcription Factor Assay kit (#10007889).

Immunostaining and image processing and quantification

Fixed primary neurons were washed, permeablized, blocked, and incubated in primary antibody solution overnight at 4°C (Mouse anti-MAP2, Millipore, #MAB3418, 1: 2000; Rabbit anti-Synaptophysin, Synaptic Systems, #101 002, 1:2000; Mouse anti-GluR1, Millipore, #MAB2263, 1:500; Rabbit anti-VGluT1, Synaptic Systems, #135 302, 1: 1000; Mouse anti-VGAT, Synaptic systems, #131 011, 1: 1000; Mouse anti-GFAP, Millipore, #MAB3402, 1:2000; Rabbit anti-p65, Cell signaling, #8242, 1:100). For immunostaining of surface GluR1, neurons were incubated with diluted anti-GluR1 antibody (1:100) at 37°C for 5 min before fixation. Coverslips were mounted in DAPI solution after washing and secondary antibody incubation.

Synapses were recognized as puncta positive for presynaptic markers (Syn, VGluT1, or VGAT) in proximity to the dendritic marker MAP2. NeuronJ (Meijering, 2004) and

Advanced Sholl analysis plugins of ImageJ were used to calculate total dendritic length and dendritic complexity. ImageJ was used to measure GluR1 fluorescent intensity over the whole cell surface, blots of surface GluR1, and synaptic density which equals number of positive puncta divided by length of the dendrite. Adobe Photoshop was used to measure GluR1 expression in Syn^+ puncta using Z-stack images of both GluR1 and Syn channels. Spine density was calculated as number of spines divided by dendritic length using the 3D renderings of AAV-GFP-infected neuronal dendritic spines reconstructed by Neurolucida (MBF Bioscience) (See Video S1). Classification and quantification of frequency and density of different spine types were performed using IMARIS software (Bitplane). AAV-GCaMP6s-infected neurons and slices were imaged using EVOS fluorescence microscope (AMG) at 10× magnification. Images were processed by Adobe Photoshop to measure GFP fluorescence.

Electrophysiology

Hippocampal cultures were transferred to a recording chamber perfused with ACSF solution containing 1 μM TTX, and 100 μM picrotoxin. mEPSCs were recorded using electrodes (Borosilicate glass, WPI) filled with whole-cell solution with a resistance of 3-6 MΩ.

Field recordings of Schaffer collateral LTP was performed as described (Peethumnongsin et al., 2010; Polito et al., 2014). Stimulation of Schaffer collaterals from the CA3 region was performed with bipolar electrodes, while borosilicate glass capillary pipettes filled with recording ACSF (resistances of 2 to 3.5 MΩ) were used to record field excitatory postsynaptic potentials (fEPSPs) in the CA1 region.

Human brain tissues

Frozen frontal cortex brain tissues from control subjects and AD patients evaluated clinically and neuropathologically were obtained from the Oregon Brain Bank at Oregon Health and Science University (OHSU) in Portland, OR. The demographic information of the samples is listed in Table S1.

Statistics

All data was presented as mean ± SEM. Pairwise comparisons were analyzed using a two-tailed Student's *t*-test, while a one-way, two-way, or three-way ANOVA followed by Bonferroni post-hoc analysis, pairwise comparison, or planned means comparison was used for multiple comparisons. *P* values less than or equal to 0.05, 0.01, and 0.001 were considered statistically significant and marked as "*", "**", and "***", respectively. *P* values higher than 0.05 were considered non-significant (NS).

Supplementary Material

Refer to Web version on PubMed Central for supplementary material.

ACKNOWLEDGMENTS

We are grateful to N. Aithmitti for expert technical assistance, B. Wang for microarray support, and members of the Zheng laboratory for stimulating discussions. We thank Drs. Costa-Mattioli (Baylor College of Medicine) and

Rupec (University of Munich) for providing the CamKIIα-Cre and *IκBα* floxed mice, respectively. This work was supported by grants from NIH (AG032051, AG020670, AG033467 and NS076117).

REFERENCES

Ahamed J, Venkatesha RT, Thangam EB, Ali H. C3a enhances nerve growth factor-induced NFAT activation and chemokine production in a human mast cell line, HMC-1. J. Immunol. 2004; 172:6961–6968. [PubMed: 15153516]

Ahn HJ, Hernandez CM, Levenson JM, Lubin FD, Liou HC, Sweatt JD. c-Rel, an NF-κB family transcription factor, is required for hippocampal long-term synaptic plasticity and memory formation. Learn. Mem. 2008; 15:539–549. [PubMed: 18626097]

Bajenaru ML, Zhu Y, Hedrick NM, Donahoe J, Parada LF, Gutmann DH. Astrocyte-specific inactivation of the neurofibromatosis 1 gene (NF1) is insufficient for astrocytoma formation. Mol. Cell. Biol. 2002; 22:5100–5113. [PubMed: 12077339]

Baltimore D. NF-κB is 25. Nat. Immunol. 2011; 12:683–685. [PubMed: 21772275]

Beattie EC, Stellwagen D, Morishita W, Bresnahan JC, Ha BK, Von Zastrow M, Beattie MS, Malenka RC. Control of synaptic strength by glial TNFα. Science. 2002; 295:2282–2285. [PubMed: 11910117]

Beg AA, Sha WC, Bronson RT, Baltimore D. Constitutive NF-κB activation, enhanced granulopoiesis, and neonatal lethality in IκBα-deficient mice. Genes. Dev. 1995; 9:2736–2746. [PubMed: 7590249]

Bénard M, Raoult E, Vaudry D, Leprince J, Falluel-Morel A, Gonzalez BJ, Galas L, Vaudry H, Fontaine M. Role of complement anaphylatoxin receptors (C3aR, C5aR) in the development of the rat cerebellum. Mol. Immunol. 2008; 45:3767–3774. [PubMed: 18635264]

Benoit ME, Tenner AJ. Complement protein C1q-mediated neuroprotection is correlated with regulation of neuronal gene and microRNA expression. J. Neurosci. 2011; 31:3459–3469. [PubMed: 21368058]

Blondeau N, Widmann C, Lazdunski M, Heurteaux C. Activation of the nuclear factor-κB is a key event in brain tolerance. J. Neurosci. 2001; 21:4668–4677. [PubMed: 11425894]

Boersma MCH, Dresselhaus EC, De Biase LM, Mihalas AB, Bergles DE, Meffert MK. A requirement for nuclear factor-κB in developmental and plasticity-associated synaptogenesis. J. Neurosci. 2011; 31:5414–5425. [PubMed: 21471377]

Chen TW, Wardill TJ, Sun Y, Pulver SR, Renninger SL, Baohan A, Schreiter ER, Kerr RA, Orger MB, Jayaraman V, et al. Ultrasensitive fluorescent proteins for imaging neuronal activity. Nature. 2013; 499:295–300. [PubMed: 23868258]

Chiao PJ, Miyamoto S, Verma IM. Autoregulation of IκBα activity. Proc. Natl. Acad. Sci. U. S. A. 1994; 91:28–32. [PubMed: 8278379]

Coulter DA, Eid T. Astrocytic regulation of glutamate homeostasis in epilepsy. Glia. 2012; 60:1215–1226. [PubMed: 22592998]

Derkach VA, Oh MC, Guire ES, Soderling TR. Regulatory mechanisms of AMPA receptors in synaptic plasticity. Nat. Rev. Neurosci. 2007; 8:101–113. [PubMed: 17237803]

Dragatsis I, Zeitlin S. CaMKIIα-Cre transgene expression and recombination patterns in the mouse brain. Genesis. 2000; 26:133–135. [PubMed: 10686608]

Drögemüller K, Helmuth U, Brunn A, Sakowicz-Burkiewicz M, Gutmann DH, Mueller W, Deckert M, Schlüter D. Astrocyte gp130 expression is critical for the control of toxoplasma encephalitis. J. Immunol. 2008; 181:2683–2693. [PubMed: 18684959]

Farber K, Cheung G, Mitchell D, Wallis R, Weihe E, Schwaeble W, Kettenmann H. C1q, the recognition subcomponent of the classical pathway of complement, drives microglial activation. J. Neurosci. Res. 2009; 87:644–652. [PubMed: 18831010]

Fonseca MI, Ager RR, Chu SH, Yazan O, Sanderson SD, LaFerla FM, Taylor SM, Woodruff TM, Tenner AJ. Treatment with a C5aR antagonist decreases pathology and enhances behavioral performance in murine models of Alzheimer's disease. J. Immunol. 2009; 183:1375–1383. [PubMed: 19561098]

Fowler SW, Chiang AC, Savjani RR, Larson ME, Sherman MA, Schuler DR, Cirrito JR, Lesne SE, Jankowsky JL. Genetic modulation of soluble Aβ rescues cognitive and synaptic impairment in a mouse model of Alzheimer's disease. J. Neurosci. 2014; 34:7871–7885. [PubMed: 24899710]

Gasque P, Dean YD, McGreal EP, VanBeek J, Morgan BP. Complement components of the innate immune system in health and disease in the CNS. Immunopharmacology. 2000; 49:171–186. [PubMed: 10904116]

Gerondakis S, Grumont R, Gugasyan R, Wong L, Isomura I, Ho W, Banerjee A. Unravelling the complexities of the NF-κB signalling pathway using mouse knockout and transgenic models. Oncogene. 2006; 25:6781–6799. [PubMed: 17072328]

Gogolla N, Galimberti I, DePaola V, Caroni P. Preparation of organotypic hippocampal slice cultures for long-term live imaging. Nat. Protoc. 2006; 1:1165–1171. [PubMed: 17406399]

Guerrini L, Molteni A, Wirth T, Kistler B, Blasi F. Glutamate-dependent activation of NF-κB during mouse cerebellum development. J. Neurosci. 1997; 17:6057–6063. [PubMed: 9236217]

Hanafusa N, Sogabe H, Yamada K, Wada T, Fujita T, Nangaku M. Contribution of genetically engineered animals to the analyses of complement in the pathogenesis of nephritis. Nephrol. Dial. Transplant 17 Suppl. 2002; 9:34–36.

Herkenham M, Rathore P, Brown P, Listwak S. Cautionary notes on the use of NF-κB p65 and p50 antibodies for CNS studies. J. Neuroinflammation. 2011; 8:141. [PubMed: 21999414]

Holers VM. Complement and its receptors: new insights into human disease. Annu. Rev. Immunol. 2014; 32:433–459. [PubMed: 24499275]

Hsiao HY, Chen YC, Chen HM, Tu PH, Chern Y. A critical role of astrocyte-mediated nuclear factor-κB-dependent inflammation in Huntington's disease. Hum. Mol. Genet. 2013; 22:1826–1842. [PubMed: 23372043]

Humbles AA, Lu B, Nilsson CA, Lilly C, Israel E, Fujiwara Y, Gerard NP, Gerard C. A role for the C3a anaphylatoxin receptor in the effector phase of asthma. Nature. 2000; 406:998–1001. [PubMed: 10984054]

Hunot S, Brugg B, Ricard D, Michel PP, Muriel MP, Ruberg M, Faucheux BA, Agid Y, Hirsch EC. Nuclear translocation of NF-κB is increased in dopaminergic neurons of patients with parkinson disease. Proc. Natl. Acad. Sci. U. S. A. 1997; 94:7531–7536. [PubMed: 9207126]

Jankowsky JL, Slunt HH, Gonzales V, Savonenko AV, Wen JC, Jenkins NA, Copeland NG, Younkin LH, Lester HA, Younkin SG, Borchelt DR. Persistent amyloidosis following suppression of Aβ production in a transgenic model of Alzheimer disease. PLoS. Med. 2005; 2:e355. [PubMed: 16279840]

Kaltschmidt B, Deller T, Frotscher M, Kaltschmidt C. Ultrastructural localization of activated NF-κB in granule cells of the rat fascia dentata. Neuroreport. 2000; 11:839–844. [PubMed: 10757530]

Kaltschmidt B, Ndiaye D, Korte M, Pothion S, Arbibe L, Prullage M, Pfeiffer J, Lindecke A, Staiger V, Israel A, et al. NF-κB regulates spatial memory formation and synaptic plasticity through protein kinase A/CREB signaling. Mol. Cell. Biol. 2006; 26:2936–2946. [PubMed: 16581769]

Kaltschmidt B, Uherek M, Volk B, Baeuerle PA, Kaltschmidt C. Transcription factor NF-κB is activated in primary neurons by amyloid beta peptides and in neurons surrounding early plaques from patients with Alzheimer disease. Proc. Natl. Acad. Sci. U. S. A. 1997; 94:2642–2647. [PubMed: 9122249]

Kaltschmidt C, Kaltschmidt B, Baeuerle PA. Brain synapses contain inducible forms of the transcription factor NF-κB. Mech. Dev. 1993; 43:135–147. [PubMed: 8297787]

Kaltschmidt C, Kaltschmidt B, Baeuerle PA. Stimulation of ionotropic glutamate receptors activates transcription factor NF-κB in primary neurons. Proc. Natl. Acad. Sci. U. S. A. 1995; 92:9618–9622. [PubMed: 7568184]

Kaltschmidt C, Kaltschmidt B, Neumann H, Wekerle H, Baeuerle PA. Constitutive NF-κB activity in neurons. Mol. Cell. Biol. 1994; 14:3981–3992. [PubMed: 8196637]

Kassed CA, Willing AE, Garbuzova-Davis S, Sanberg PR, Pennypacker KR. Lack of NF-κB p50 exacerbates degeneration of hippocampal neurons after chemical exposure and impairs learning. Exp. Neurol. 2002; 176:277–288. [PubMed: 12359170]

Klement J, Rice N, Car B, Abbondanzo S, Powers G, Bhatt P, Chen C, Rosen C, Stewart C. IκBα deficiency results in a sustained NF-κB response and severe widespread dermatitis in mice. Mol. Cell. Biol. 1996; 16:2341–2349. [PubMed: 8628301]

Koo J, Russo S, Ferguson D, Nestler E, Duman R. Nuclear factor-κB is a critical mediator of stress-impaired neurogenesis and depressive behavior. Proc. Natl. Acad. Sci. U. S. A. 2010; 107:2669–2674. [PubMed: 20133768]

Kyritsis N, Kizil C, Brand M. Neuroinflammation and central nervous system regeneration in vertebrates. Trends. Cell. Biol. 2014; 24:128–135. [PubMed: 24029244]

LaFerla FM. Calcium dyshomeostasis and intracellular signalling in Alzheimer's disease. Nat Rev Neurosci. 2002; 3:862–872. [PubMed: 12415294]

Lalo U, Palygin O, Rasooli-Nejad S, Andrew J, Haydon PG, Pankratov Y. Exocytosis of ATP from astrocytes modulates phasic and tonic inhibition in the neocortex. PLoS. Biol. 2014; 12:e1001747. [PubMed: 24409095]

Leinhase I, Schmidt OI, Thurman JM, Hossini AM, Rozanski M, Taha ME, Scheffler A, John T, Smith WR, Holers VM, Stahel PF. Pharmacological complement inhibition at the C3 convertase level promotes neuronal survival, neuroprotective intracerebral gene expression, and neurological outcome after traumatic brain injury. Exp. Neurol. 2006; 199:454–464. [PubMed: 16545803]

Levenson JM, Choi S, Lee SY, Cao YA, Ahn HJ, Worley KC, Pizzi M, Liou HC, Sweatt JD. A bioinformatics analysis of memory consolidation reveals involvement of the transcription factor c-rel. J. Neurosci. 2004; 24:3933–3943. [PubMed: 15102909]

Lian H, Shim DJ, Gaddam SS, Rodriguez-Rivera J, Bitner BR, Pautler RG, Robertson CS, Zheng H. IκBα deficiency in brain leads to elevated basal neuroinflammation and attenuated response following traumatic brain injury: implications for functional recovery. Mol. Neurodegener. 2012; 7:47. [PubMed: 22992283]

Lucin KM, Wyss-Coray T. Immune activation in brain aging and neurodegeneration: too much or too little? Neuron. 2009; 64:110–122. [PubMed: 19840553]

Mao X, Moerman-Herzog A, Chen Y, Barger S. Unique aspects of transcriptional regulation in neurons - nuances in NFκB and Sp1-related factors. J. Neuroinflammation. 2009; 6:16. [PubMed: 19450264]

Maranto J, Rappaport J, Datta PK. Regulation of complement component C3 in astrocytes by IL-1β and morphine. J. Neuroimmune. Pharmacol. 2008; 3:43–51. [PubMed: 18247123]

Maranto J, Rappaport J, Datta PK. Role of C/EBP-β, p38 MAPK, and MKK6 in IL-1β-mediated C3 gene regulation in astrocytes. J. Cell. Biochem. 2011; 112:1168–1175. [PubMed: 21308746]

Mattson MP. Calcium and neurodegeneration. Aging. Cell. 2007; 6:337–350. [PubMed: 17328689]

Mattson MP, Culmsee C, Yu Z, Camandola S. Roles of nuclear factor κB in neuronal survival and plasticity. J. Neurochem. 2000; 74:443–456. [PubMed: 10646495]

Mattson MP, Meffert MK. Roles for NF-κB in nerve cell survival, plasticity, and disease. Cell. Death. Differ. 2006; 13:852–860. [PubMed: 16397579]

Meffert MK, Chang JM, Wiltgen BJ, Fanselow MS, Baltimore D. NF-κB functions in synaptic signaling and behavior. Nat. Neurosci. 2003; 6:1072–1078. [PubMed: 12947408]

Meijering E, Jacob M, Sarria J-CF, Steiner P, Hirling H, Unser M. Design and validation of a tool for neurite tracing and analysis in fluorescence microscopy images. Cytometry. A. 2004; 58:167–176. [PubMed: 15057970]

Moon MR, Parikh AA, Pritts TA, Fischer JE, Cottongim S, Szabo C, Salzman AL, Hasselgren PO. Complement component C3 production in IL-1β-stimulated human intestinal epithelial cells is blocked by NF-κB inhibitors and by transfection with ser 32/36 mutant IκBα. J. Surg. Res. 1999; 82:48–55. [PubMed: 10068525]

Mori T, Koyama N, Arendash GW, Horikoshi-Sakuraba Y, Tan J, Town T. Overexpression of human S100B exacerbates cerebral amyloidosis and gliosis in the Tg2576 mouse model of Alzheimer's disease. Glia. 2010; 58:300–314. [PubMed: 19705461]

Murakami Y, Imamichi T, Nagasawa S. Characterization of C3a anaphylatoxin receptor on guinea-pig macrophages. Immunology. 1993; 79:633–638. [PubMed: 8406589]

Nataf S, Stahel PF, Davoust N, Barnum SR. Complement anaphylatoxin receptors on neurons: new tricks for old receptors? Trends. Neurosci. 1999; 22:397–402. [PubMed: 10441300]

Oeckinghaus A, Ghosh S. The NF-κB family of transcription factors and its regulation. Cold. Spring. Harb. Perspect. Biol. 2009; 1:a000034. [PubMed: 20066092]

Peethumnongsin E, Yang L, Kallhoff-Munoz V, Hu L, Takashima A, Pautler RG, Zheng H. Convergence of presenilin- and tau-mediated pathways on axonal trafficking and neuronal function. J. Neurosci. 2010; 30:13409–13418. [PubMed: 20926667]

Peng B, Ling J, Lee AJ, Wang Z, Chang Z, Jin W, Kang Y, Zhang R, Shim D, Wang H, et al. Defective feedback regulation of NF-κB underlies Sjogren's syndrome in mice with mutated κB enhancers of the IκBα promoter. Proc. Natl. Acad. Sci. U. S. A. 2010; 107:15193–15198. [PubMed: 20696914]

Pizzi M, Spano P. Distinct roles of diverse nuclear factor-κB complexes in neuropathological mechanisms. Eur. J. Pharmacology. 2006; 545:22–28.

Polito VA, Li H, Martini-Stoica H, Wang B, Yang L, Xu Y, Swartzlander DB, Palmieri M, di Ronza A, Lee VM, et al. Selective clearance of aberrant tau proteins and rescue of neurotoxicity by transcription factor EB. EMBO. Mol. Med. 2014; 6:1142–1160. [PubMed: 25069841]

Rahpeymai Y, Hietala MA, Wilhelmsson U, Fotheringham A, Davies I, Nilsson AK, Zwirner J, Wetsel RA, Gerard C, Pekny M, Pekna M. Complement: a novel factor in basal and ischemia-induced neurogenesis. EMBO. J. 2006; 25:1364–1374. [PubMed: 16498410]

Ricklin D, Lambris JD. Complement in immune and inflammatory disorders: pathophysiological mechanisms. J. Immunol. 2013; 190:3831–3838. [PubMed: 23564577]

Sayah S, Jauneau AC, Patte C, Tonon MC, Vaudry H, Fontaine M. Two different transduction pathways are activated by C3a and C5a anaphylatoxins on astrocytes. Mol. Brain. Res. 2003; 112:53–60. [PubMed: 12670702]

Seifert G, Steinhauser C. Neuron-astrocyte signaling and epilepsy. Exp. Neurol. 2013; 244:4–10. [PubMed: 21925173]

Sheppard PW, Sun X, Emery JF, Giffard RG, Khammash M. Quantitative characterization and analysis of the dynamic NF-κB response in microglia. BMC. Bioinformatics. 2011; 12:276. [PubMed: 21729324]

Shim DJ, Yang L, Reed JG, Noebels JL, Chiao PJ, Zheng H. Disruption of the NF-κB/IκBα autoinhibitory loop improves cognitive performance and promotes hyperexcitability of hippocampal neurons. Mol. Neurodegener. 2011; 6:42. [PubMed: 21663635]

Shinjyo N, Ståhlberg A, Dragunow M, Pekny M, Pekna M. Complement-derived anaphylatoxin C3a regulates in vitro differentiation and migration of neural progenitor cells. Stem. Cells. 2009; 27:2824–2832. [PubMed: 19785034]

Simakajornboon N, Gozal E, Gozal D. Developmental patterns of NF-κB activation during acute hypoxia in the caudal brainstem of the rat. Brain. Res. Dev. Brain. Res. 2001; 127:175–183.

Song I, Huganir RL. Regulation of AMPA receptors during synaptic plasticity. Trends. Neurosci. 2002; 25:578–588. [PubMed: 12392933]

Stellwagen D, Malenka RC. Synaptic scaling mediated by glial TNFα. Nature. 2006; 440:1054–1059. [PubMed: 16547515]

Stevens B, Allen NJ, Vazquez LE, Howell GR, Christopherson KS, Nouri N, Micheva KD, Mehalow AK, Huberman AD, Stafford B, et al. The classical complement cascade mediates CNS synapse elimination. Cell. 2007; 131:1164–1178. [PubMed: 18083105]

Stine WB Jr. Dahlgren KN, Krafft GA, LaDu MJ. In vitro characterization of conditions for amyloid-β peptide oligomerization and fibrillogenesis. J. Biol. Chem. 2003; 278:11612–11622. [PubMed: 12499373]

Vik DP, Amiguet P, Moffat GJ, Fey M, Amiguet-Barras F, Wetsel RA, Tack BF. Structural features of the human C3 gene: intron/exon organization, transcriptional start site, and promoter region sequence. Biochemistry. 1991; 30:1080–1085. [PubMed: 1703437]

Woodruff TM, Costantini KJ, Crane JW, Atkin JD, Monk PN, Taylor SM, Noakes PG. The complement factor C5a contributes to pathology in a rat model of amyotrophic lateral sclerosis. J. Immunol. 2008; 181:8727–8734. [PubMed: 19050293]

Wyss-Coray T, Rogers J. Inflammation in Alzheimer disease-a brief review of the basic science and clinical literature. Cold Spring Harb Perspect Med. 2012; 2:a006346. [PubMed: 22315714]

Yamada KA. Modulating excitatory synaptic neurotransmission: potential treatment for neurological disease? Neurobiol. Dis. 1998; 5:67–80. [PubMed: 9746904]

Yang L, Wang Z, Wang B, Justice NJ, Zheng H. Amyloid precursor protein regulates Cav1.2 L-type calcium channel levels and function to influence GABAergic short-term plasticity. J. Neurosci. 2009; 29:15660–15668. [PubMed: 20016080]

Zhang J, Malik A, Choi HB, Ko RW, Dissing-Olesen L, Macvicar BA. Microglial CR3 Activation Triggers Long-Term Synaptic Depression in the Hippocampus via NADPH Oxidase. Neuron. 2014; 82:195–207. [PubMed: 24631344]

Zipfel PF, Skerka C. Complement regulators and inhibitory proteins. Nat. Rev. Immunol. 2009; 9:729–740. [PubMed: 19730437]

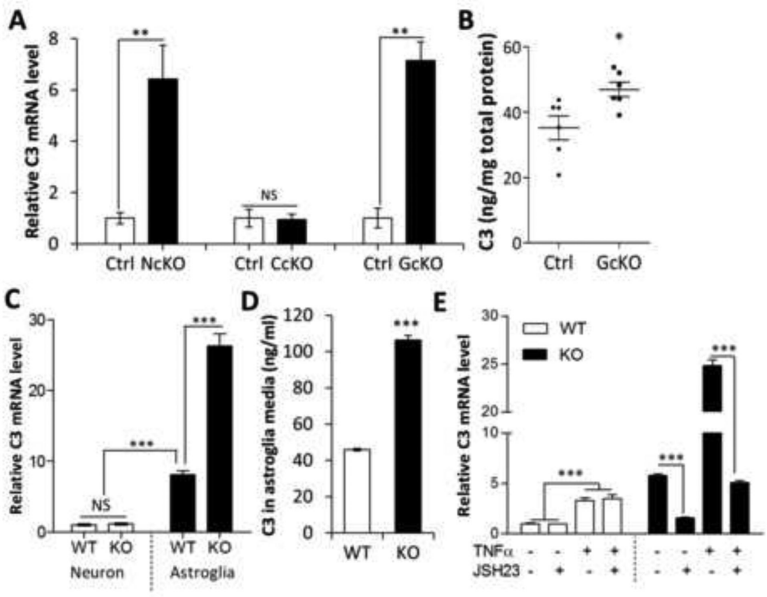

Figure 1. C3 is overexpressed in IκBα-deficient astroglia

(A) Quantitative RT-PCR measurement of C3 mRNA expression in hippocampal samples of 2-month-old *Nestin-Cre; IκBα$^{fl/-}$* (NcKO), *CamKIIα-Cre; IκBα$^{fl/-}$* (CcKO), and *GFAP-Cre; IκBα$^{fl/-}$* (GcKO) mice and their littermate controls (Ctrl). (B) C3 protein levels in GcKO and Ctrl hippocampi measured by ELISA. (C) C3 mRNA levels in wild-type (WT) and IκBα knockout (KO) primary neurons or astroglia. (D) ELISA quantification of C3 protein levels in conditioned media of WT or IκBα KO astroglial cultures. (E) C3 mRNA expression in WT or IκBα KO astroglial cultures treated with different combinations of TNFα (50 ng/ml) or NFκB inhibitor JSH23 (20 μM). N=3 per group per experiment except N=6 in (B). A, B, and D: Student's *t*-test; C: Two-way ANOVA followed by pairwise comparison. E: Three-way ANOVA followed by pairwise comparison. **P* < 0.05; ***P* < 0.01; ****P* < 0.001; NS: non-significant. See also Figure S1.

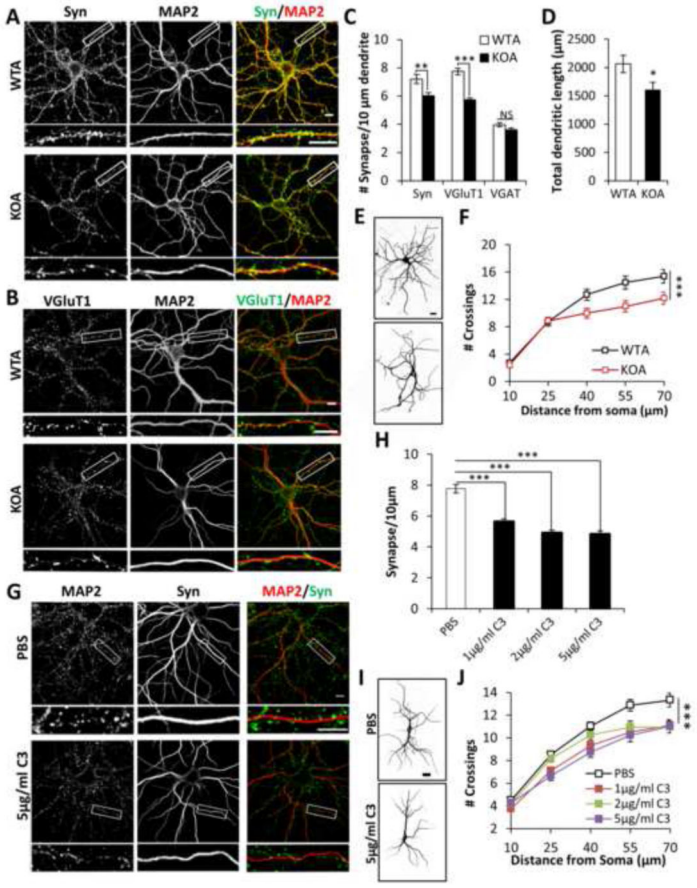

Figure 2. Astroglial C3 alters synaptic and dendritic morphology

(A) Double-immunostaining of wild-type or IκBα KO astroglia (WTA or KOA) co-cultured neurons with anti-synaptophysin (Syn) and anti-MAP2 (MAP2) antibodies. (B) Same as (A) except that anti-VGluT1 (VGluT1) antibody was used instead of Syn. Images underneath each panel are enlarged view of the bracketed areas. (C) Quantification of number of $Syn^{+}MAP2^{+}$, $VGluT1^{+}MAP2^{+}$ or $VGAT^{+}MAP2^{+}$ synaptic puncta per 10 μm of dendrite in WTA and KOA co-cultured neurons. $N_{WTA\ Syn}$=31; $N_{KOA\ Syn}$=28; $N_{WTA\ VGluT1}$=57; $N_{KOA\ VGluT1}$=52; $N_{WTA\ VGAT}$=45; $N_{KOA\ VGAT}$=52. (D) Quantification of total MAP2-positive dendritic length in WTA and KOA co-cultured neurons. N_{WTA}=38; N_{KOA}=42. (E) Representative dendritic structure, (F) Quantification of dendritic complexity of WTA and KOA co-cultured neurons by Sholl analysis. N_{WTA}=39; N_{KOA}=44. (G) Double staining of Syn and MAP2 of WT neurons treated with vehicle (PBS) or 5 μg/ml C3. (H) Quantified synaptic density of neurons treated with PBS or C3 at 1, 2, or 5 μg/ml. N_{PBS}=36; $N_{1\mu g/ml}$=33; $N_{2\mu g/ml}$=37; $N_{5\mu g/ml}$=29. (I) Representative dendritic structures of WT neurons treated with PBS or 5 μg/ml C3. (J) Dendritic complexity quantification of WT neurons treated with PBS or C3 at 1, 2, and 5 μg/ml. N_{PBS}=116; $N_{1\mu g/ml}$=66; $N_{2\mu g/ml}$=53; $N_{5\mu g/ml}$=68. Scale bar: 10 μm in (A, B, G) and 20 μm in (E, I). C and D: Student's *t*-test. F: Two-way ANOVA. H: One-way ANOVA followed by Bonferroni post-hoc analysis. J: Two-way ANOVA followed by Bonferroni post-hoc analysis. **P* < 0.05; ***P* < 0.01; ****P* < 0.001; NS: non-significant. See also Figure S2.

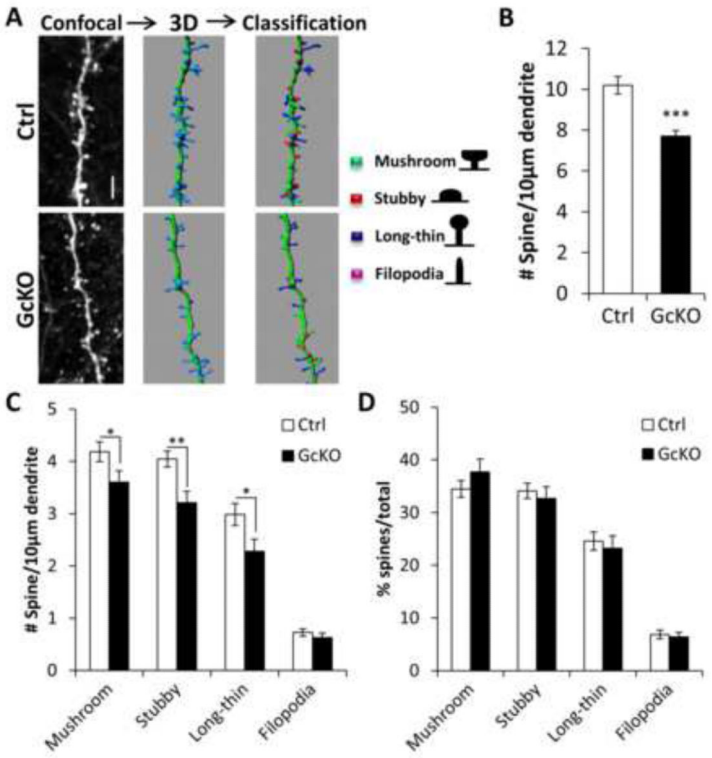

Figure 3. Impaired dendritic morphology in astroglial IκBα-deficient (GcKO) mice

(A) Schematic representation of the steps taken for dendritic spine analysis in vivo. Four-month-old littermate control (Ctrl) and GcKO mouse brains were stereotaxically injected with AAV-GFP virus followed by measurement of spine density 3 weeks later. IMARIS was used to reconstruct the 3D renderings of the spines on dendrites based on confocal images of GFP-positive neurons and classify the four spine types (mushroom, stubby, long-thin and filopodia). (B) Total spine density in Ctrl and GcKO mouse brains. N_{Ctrl}=25; N_{GcKO}=22. (C) Density of each of the four spine types in Ctrl and GcKO mouse brains. N_{Ctrl}=39; N_{GcKO}=31. (D) Frequency of each spine types. Scale bar: 5 μm. Dendritic segments were derived from 3 animals/group. Student's *t*-test. **P* < 0.05; ***P* < 0.01; ****P* < 0.001. See also Video S1 and Figure S3.

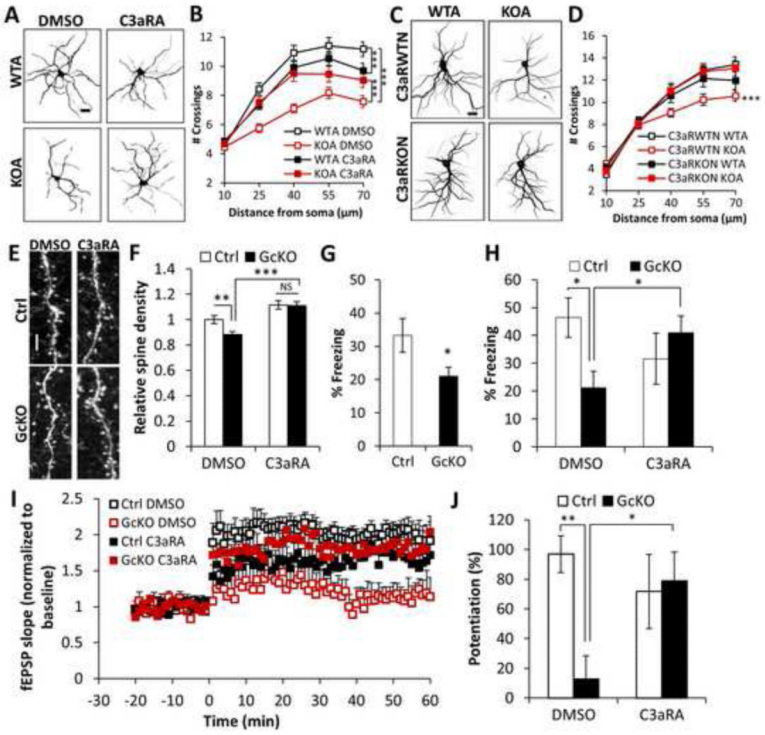

Figure 4. Neuronal C3aR mediates dendritic morphology and network function

(A) Representative images of MAP2-positive dendritic structures in wild-type or IκBα KO astroglia (WTA or KOA) co-cultured neurons treated with DMSO or 1 μM C3aRA for 4 days. (B) Sholl analysis of dendritic complexity of WTA or KOA co-cultured neurons treated with DMSO or C3aRA. $N_{WTA\ DMSO}$=47; $N_{KOA\ DMSO}$=55; $N_{WTA\ C3aRA}$=63; $N_{KOA\ C3aRA}$=57. (C) Representative MAP2-positive dendrites of C3aR wild-type (C3aRWTN) or knockout (C3aRKON) neurons co-cultured with IκBα WT or KO astroglia (WTA or KOA). (D) Sholl analysis of dendritic complexity of WTA or KOA co-cultured C3aRWTN or C3aRKON neurons. $N_{C3aRWTN\ WTA}$=46; $N_{C3aRKOA\ WTA}$=51; $N_{C3aRWTN\ KOA}$=44; $N_{C3aRKOA\ KOA}$=46. (E) Representative dendritic spines in 10 month-old Ctrl or GcKO mouse brains treated with DMSO or C3aRA (1 mg/kg i.p.) for 3 weeks. (F) Quantification of spine density in Ctrl or GcKO mouse brains treated with DMSO or C3aRA. $N_{Ctrl\ DMSO}$=69; $N_{GcKO\ DMSO}$=80; $N_{Ctrl\ C3aRA}$=41; $N_{GcKO\ C3aRA}$=43. Dendritic segments from 3 animals/group were selected for spine density quantification. (G) Reduced contextual freezing in GcKO mice N_{Ctrl}=14; N_{GcKO}=18. (H) Rescue of contextual memory defects of GcKO mice by C3aRA treatment. DMSO: vehicle treated controls. $N_{Ctrl\ DMSO}$=6; $N_{GcKO\ DMSO}$=7; $N_{Ctrl\ C3aRA}$=8; $N_{GcKO\ C3aRA}$=6. (I) Slope of field excitatory postsynaptic potential (fEPSP) in response to theta burst stimulation delivered to the Schaffer collateral pathway from Ctrl or GcKO mice treated with DMSO or C3aRA. (J) Quantification of average fEPSP slope in the last 10 minutes. $N_{Ctrl\ DMSO}$=6; $N_{GcKO\ DMSO}$=5; $N_{Ctrl\ C3aRA}$=8; $N_{GcKO\ C3aRA}$=6. Scale bar: 20 μm in (A, C) and 10 μm in (E). B and D: Three-way ANOVA followed by pairwise comparison; F, H, and J: Two-way ANOVA followed by pairwise comparison. G: Student's *t*-test. **P* < 0.05; ***P* < 0.01; ****P* < 0.001; NS: non-significant. See also Figure S4.

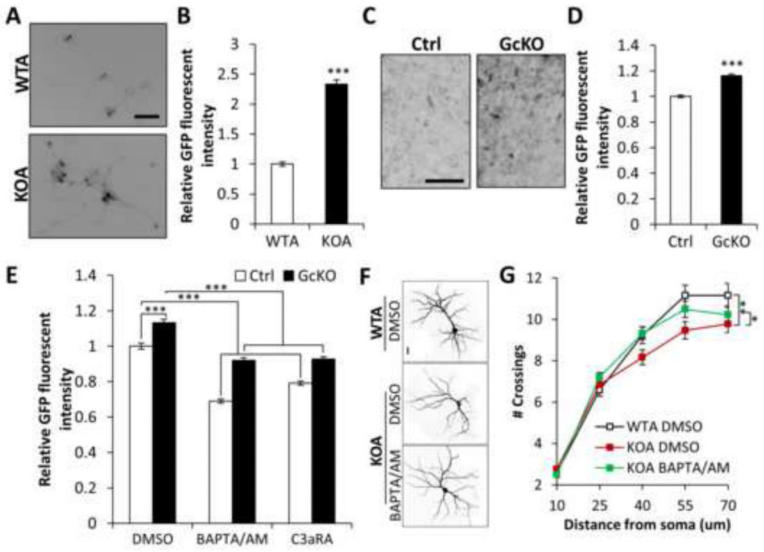

Figure 5. Astroglial NFκB activation leads to aberrant intraneuronal calcium

(A) Representative images of GCaMP fluorescence in AAV-GCaMP6s-infected neurons co-cultured with wild-type or IκBα KO astroglia (WTA or KOA). (B) Mean GFP fluorescence in co-cultured neurons. N_{WTA}=221; N_{KOA}=234. (C) Representative GFP fluorescence in Ctrl or GcKO derived organotypic hippocampal slice cultures infected with AAV-GCaMP6s. (D) Quantification of basal GFP fluorescence intensity. N=65/ group. (E) Mean GCaMP fluorescence of Ctrl and GcKO slice cultures treated with DMSO, 10 μM C3aRA or 50 μM BAPTA/AM. $N_{Ctrl\ DMSO}$=103; $N_{GcKO\ DMSO}$=104; $N_{Ctrl\ BAPTA/AM}$=60; $N_{GcKO\ BAPTA/AM=}$60; $N_{Ctrl\ C3aRA}$=180; $N_{GcKO\ C3aRA}$=104. (F) Representative images of MAP2-positive dendritic morphologies in WTA or KOA co-cultured neurons treated with DMSO or 1 μM BAPTA/AM for 4 days. (G) Sholl analysis of dendritic complexity of WTA or KOA co-cultured neurons treated with DMSO or BAPTA/AM. $N_{WTA\ DMSO}$=52; $N_{KOA\ DMSO}$=62; $N_{KOA\ BAPTA/AM}$=70. Scale bar: 50 μm in (A), 100 μm in (C), 20 μm in (F). B and D: Student's *t*-test; E: Two-way ANOVA followed by Bonferroni post-hoc analysis; G: Three-way ANOVA followed by pairwise comparison. **P* < 0.05; ***P* < 0.01; ****P* < 0.001. See also Video S2.

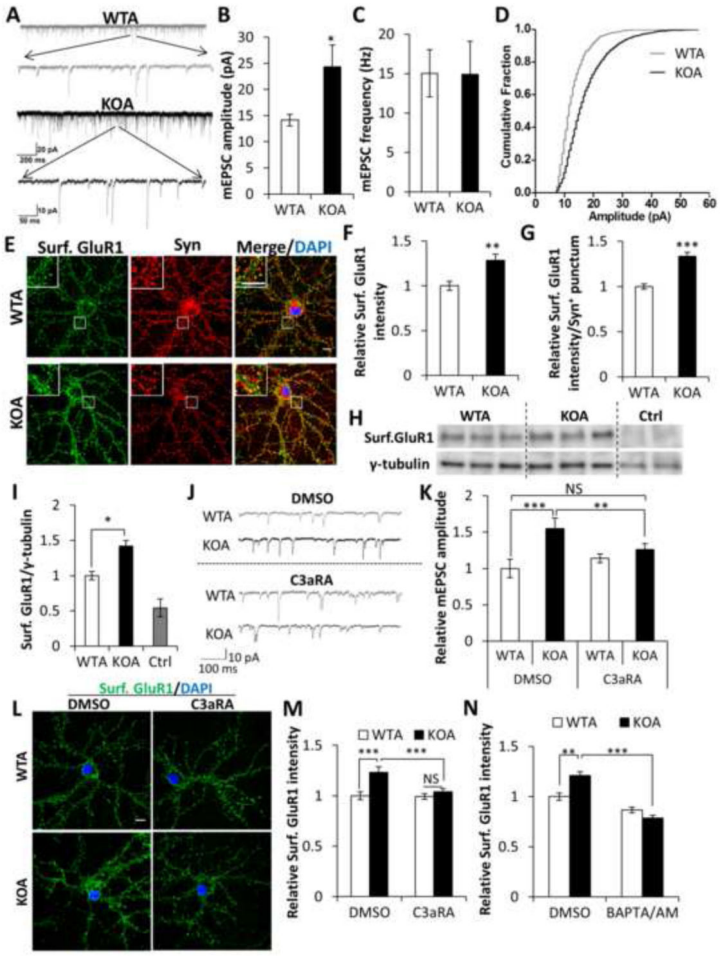

Figure 6. C3aR and intraneuronal calcium mediates excitatory synaptic transmission and surface AMPAR expression

(A) Example mEPSC traces of wild-type or *IκBα* KO astroglia (WTA or KOA) co-cultured neurons. (B) Increased mEPSC amplitude in KOA neurons compared to WTA controls. (C) No differences of mEPSC frequency between WTA and KOA cultures. (D) mEPSC amplitude fractionation curve of WTA and KOA neurons. N_{WTA}=13; N_{KOA}=14. (E) Representative images of co-cultured WTA and KOA neurons stained against surface GluR1 (Surf. GluR1) and synaptophysin (Syn) and counter-stained with DAPI. Inset: Enlarged images of the bracketed areas. (F) Relative fluorescence intensity of Surf. GluR1 over whole cell surface (N_{WTA}=20; N_{KOA}=19) and (G) Relative fluorescence intensity of Surf. GluR1 in Syn^{+} puncta (N_{WTA}=60,000; N_{KOA}=45,000). (H) Blots of surface GluR1 in co-cultured neuronal lysates. Cell surface protein samples were prepared by surface biotinylation. Ctrl lanes are samples from neurons without biotin incubation. Loading was quantified by blotting with an anti-γ-tubulin antibody in cell lysates before neutravidin pulldown. (I) Quantification of the blot in (H). (J) Sample mEPSC traces of wild-type or IκBα KO astroglia (WTA or KOA) co-cultured neurons treated with DMSO or 1 μM C3aRA for 4 days. (K) Mean mEPSC amplitude of treated neurons. $N_{WTA\ DMSO}$=8; $N_{KOA\ DMSO}$=9; $N_{WTA\ C3aRA}$=12; $N_{KOA\ C3aRA}$=17. (L) Representative images of surface GluR1 staining with DAPI counter-staining in WTA or KOA neurons treated with DMSO or C3aRA. (M)

Quantification of fluorescence intensity of (L). $N_{WTA\ DMSO}$=35; $N_{KOA\ DMSO}$=31; $N_{WTA\ C3aRA}$=33; $N_{KOA\ C3aRA}$=37. (N) Quantification of Surf. GluR1 fluorescence in co-cultured neurons treated with DMSO or 1 μM BAPTA/AM for 15 min. $N_{WTA\ DMSO}$=29; $N_{KOA\ DMSO}$=24; $N_{WTA\ BAPTA/AM}$=34; $N_{KOA\ BAPTA/AM}$=31. Scale bar: 10 μm. B, C, F, G, and I: Student's *t*-test; K, M, and N: Two-way ANOVA followed by pairwise comparison. **P* < 0.05; ***P* < 0.01; ****P* < 0.001; NS: non-significant. See also Figure S5.

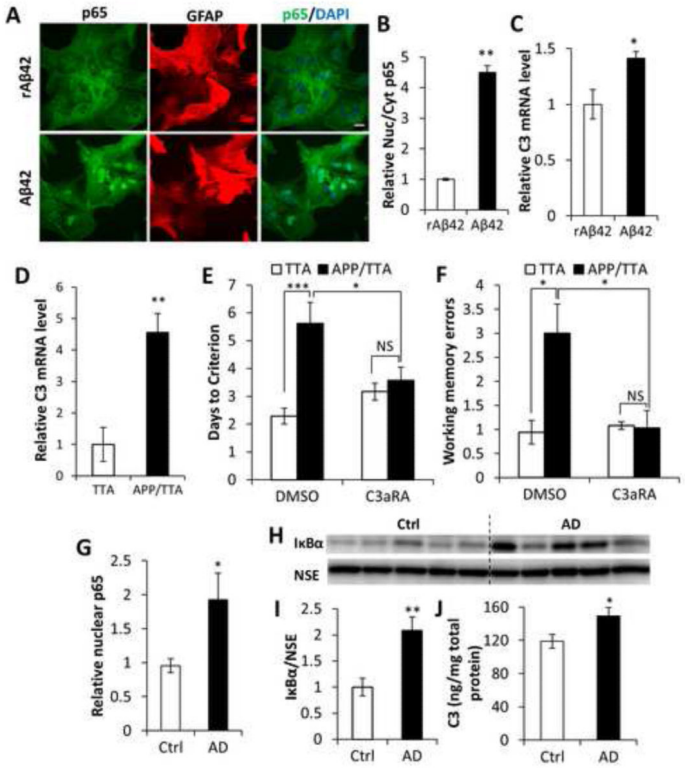

Figure 7. Activation of the NFκB/C3 in AD and beneficial effect of C3aR antagonist

(A) p65 and GFAP double-staining of primary wild-type astroglial cultures incubated with Aβ42 peptide showing p65 nuclear translation induced by Aβ42. Reverse Aβ42 peptide (rAβ42) was used as a negative control. Scale bar: 20 μm. (B) Quantification of nuclear/cytoplasmic p65 ratio. N=50 cells per group. (C) qPCR measurement of C3 mRNA expression in astroglial cultures treated with Aβ42 or rAβ42. N=3 per group. (D) C3 mRNA expression in the APP/TTA AD mouse model compared to the control TTA mice. N_{TTA}=6; $N_{APP/TTA}$=7. (E) Rescue of Morris water maze deficits in APP/TTA mice by C3aRA. $N_{TTA\ DMSO}$=7; $N_{APP/TTA\ DMSO}$=8; $N_{TTA\ C3aRA}$=6; $N_{APP/TTA\ C3aRA}$=7. (F) Rescue of radial arm water maze deficits in APP/TTA mice by C3aRA. $N_{TTA\ DMSO}$=7; $N_{APP/TTA\ DMSO}$=8; $N_{TTA\ C3aRA}$=5; $N_{APP/TTA\ C3aRA}$=7. (G) ELISA measurement of NFκB subunit p65 in nuclear fractions of human brain lysates from control subjects (Ctrl) and AD patients. N_{Ctrl}=7; N_{AD}=8. (H) Western blotting of IκBα levels in Ctrl and AD human total protein lysates. Neuron specific enolase (NSE) was used as a loading control. (I) Quantification of blots in (H). (J) C3 protein concentration in total protein lysates from control and AD brain samples. N_{Ctrl}=7; N_{AD}=8. B, C, D, G, I, and J: Student's *t*-test; E and F: Two-way ANOVA followed by pairwise comparison. **P* < 0.05; ***P* < 0.01; ****P* < 0.001; NS: non-significant. See also Table S1.